GNSS Precipitable Water Vapor from an Amazonian Rain Forest Flux Tower

DAVID K. ADAMS

Programa de Pós Graduação em Clima e Ambiente, Instituto Nacional de Pesquisas da Amazônia, and Universidade do Estado do Amazonas, Manaus, Amazonas, Brazil

RUI M. S. FERNANDES

Departamento de Informática, Universidade da Beira Interior, Covilhã, Portugal

JAIR M. F. MAIA

Escola Normal Superior, Universidade do Estado do Amazonas, and Instituto Nacional de Pesquisa da Amazônia, and the Large Scale Biosphere-Atmosphere Program, Manaus, Amazonas, Brazil

(Manuscript received 10 May 2011, in final form 25 July 2011)

ABSTRACT

Understanding the complex interactions between water vapor fields and deep convection on the mesoscale requires observational networks with high spatial (kilometers) and temporal (minutes) resolution. In the equatorial tropics, where deep convection dominates the vertical distribution of the most important greenhouse substance—water—these mesoscale networks are nonexistent. Global Navigational Satellite System (GNSS) meteorological networks offer high temporal/spatial resolution precipitable water vapor, but infrastructure exigencies are great. The authors report here on very accurate precipitable water vapor (PWV) values calculated from a GNSS receiver installed on a highly nonideal Amazon rain forest flux tower. Further experiments with a mechanically oscillating platform demonstrate that errors and biases of approximately 1 mm (2%–3% of PWV) can be expected when compared with a stable reference GNSS receiver for two different geodetic grade receivers/antennas and processing methods [GPS-Inferred Positioning System (GIPSY) and GAMIT]. The implication is that stable fixed antennas are unnecessary for accurate calculation of precipitable water vapor regardless of processing techniques or geodetic grade receiver.

1. Introduction

In tropical deep convective regimes, the distribution of water vapor is fundamental in determining outbreaks and the intensity of deep precipitating convection (see Sherwood et al. 2009 for a review). The convection–water vapor relationship is complex and multiscale, with intricate feedbacks (Grabowski and Moncrieff 2004). In particular, the vertical distribution of water vapor is directly linked to atmospheric instability/parcel energetics (Williams and Rennó 1993; Sherwood 1999; Adams and Souza 2009), the suppression of moist convection through intrusions of dry air layers (Mapes and Zuidema 1996; Parsons et al. 2000), and the shallow-to-deep convection transition (Kuang and Bretherton 2006; Wu et al. 2009). The strength of evaporatively driven downdrafts and their role in intensifying and organizing deep convection may also be tied to free tropospheric dry layers (Emanuel 1991; Grabowski and Moncrieff 2004; Roca et al. 2005) although these layers may result in opposite effects for midlatitudes (intensification) versus the tropics (suppression) (James and Markowski 2010).

Much convection–humidity research for tropical continental regions has employed high-resolution models (Khairoutdinov and Randall 2006; Grabowski et al. 2006; Wu et al. 2009; James and Markowski 2010), oftentimes with the goal of ameliorating deficiencies in convective parameterizations, particularly their poor representation of the shallow-to-deep transition and organization on the mesoscale (Betts and Jakob 2002; Bechtold et al. 2004; Grabowski et al. 2006). However, many of the feedbacks and physical processes relating deep convection to water vapor fields, which are typically not accounted for in

Corresponding author address: David K. Adams, C.E.S.T.U., Universidade do Estado do Amazonas, Av. Djalma Batista, 3578–Flores–CEP 69050-030 Manaus, Amazonas, Brazil.
E-mail: dave.k.adams@gmail.com

DOI: 10.1175/JTECH-D-11-00082.1

convective parameterizations, need to be confirmed observationally. For example, the role of cold pools in the shallow-to-deep transition and mesoscale organization is believed to be critical, but has not been fully documented observationally. Longer-term (>1 year) mesoscale meteorological networks are therefore necessary to gain insights; however, to date, only brief field campaigns have been carried out [e.g., Tropical Rainfall Measuring Mission–Large Scale Biosphere-Atmosphere Experiment in Amazonia (TRMM–LBA); Silva-Dias et al. 2002].

2. Motivations and aims of study

Existing continental tropical observational networks are inadequate for addressing mesoscale convection–humidity interactions. Radiosondes are sparsely located and temporally infrequent, (e.g., only two regular sites, separated by 1300 km, in all of Amazonia). Satellite passive IR radiometers are limited to clear-sky conditions (Divakarla et al. 2006) and satellite microwave radiometers, though more accurate, are less reliable over the land (Deeter 2007). More recently, ground-based Global Navigational Satellite System (GNSS) meteorology has offered high-frequency, all weather, precipitable water vapor (PWV) values with 1–2-mm (on the order of a few percent) accuracy relative to radiosondes and radiometers (Bevis et al. 1992; Rocken et al. 1993; Duan et al. 1996; Wolfe and Gutman 2000). The GNSS PWV methodology has been well established for many locations including the extremely moist such as the Amazon (Sapucci et al. 2007). Here the technology has proven useful in identifying propagating convective events (Kursinski et al. 2008; Adams et al. 2009) and estimating time scales for water vapor convergence (Adams et al. 2011).

PWV, although proving quite useful for theoretical studies of tropical deep convection (Muller et al. 2009; Peters and Neelin 2009), provides no vertical humidity structure. When GNSS networks are employed, 3D and 4D water vapor fields can be estimated (Flores et al. 2001; Braun et al. 2001; Bender and Raabe 2007). Efforts in Europe, Japan, and the United States have employed dense networks at both synoptic and the mesoscale for calculating 3D/4D water vapor fields (Champollion et al. 2005; Bastin et al. 2007), for PWV data assimilation into numerical weather prediction models (Gutman et al. 2004; Smith et al. 2007), and for observing convective initiation and mesoscale convective systems (Seko et al. 2004; Champollion et al. 2009). Adams et al. (2011) are presently constructing the world's only equatorial continental dense GNSS meteorological network (station separation ~5–10 km) in the central Amazon. Logistically, this region presents enormous difficulties given the stringent requirements of GNSS sites: clear-sky view, minimal multipath interference, no nearby emitting radio antennas, and stable platforms. Adequate sites in the Amazon rain forest are few. The creation of the Amazonian Dense GNSS Network (20 GNSS receivers with surface meteorological stations) motivated the use of the nonideal platform employed in this study: a 55-m meteorological rain forest flux tower (forest canopy is approximately 40 m tall), the results from which are very encouraging and are reported here.

Previous studies on oceanic platforms and moving vessels have achieved accurate PWV measurements (Chadwell and Bock 2001; Rocken et al. 2005; Fujita et al. 2008). These studies of nonideal platforms are here extended to rain forest conditions and by comparing two different models of GNSS receivers (Trimble and Topcon) and processing techniques [GAMIT and GPS-Inferred Positioning System (GIPSY)]. Clearly, employing different receivers/antennas and processing techniques necessarily precludes an exact error analysis given the impossibility of simultaneously collocating equipment in the same position. Furthermore, intrinsic errors due either to processing methods or to the equipment itself, or both, are difficult to isolate. In this sense, we attempt here only to simply set "error bounds" for very nonideal platforms further considering the utilization of different equipment and processing methods. Or, posing it succinctly, Can poor site conditions, such as an aluminum scaffolding rain forest tower, still furnish quality PWV values regardless of equipment and/or processing methods? In what follows, we detail the experiment, present the results and argue for further studies that extend GNSS meteorology into even more adverse conditions (e.g., limited sky views with permanent obstructions, high multipath environment, and proximity to powerful emitting radio antennas).

3. Experimental design, study sites, and data

a. Experimental design

To ascertain the feasibility of GNSS meteorology employing rain forest towers as platforms, two experiments were carried out. First, a GNSS receiver was placed on a 55-m rain forest flux tower. PWV was calculated and compared with values from a stable receiver 60 km away. Given that mesoscale PWV variability between the sites—and not the equipment or processing—would account for most of the variability, a second experiment was carried out. The flux tower receiver was removed and placed next to the stable reference receiver. To mimic flux tower movements, the itinerant receiver's antenna was placed on a mechanical device that oscillated at known amplitude and frequency. Our estimation of tower movements was based solely on observations and discussions with technicians and researchers. PWV was calculated again for both receivers in two configurations: 1) both rigidly fixed and 2) one oscillating, the other rigidly fixed. The first experiment was carried out from early July to mid-September 2009, during the central Amazon dry season; the second experiment between mid-September and early November 2009, the dry-to-wet transition. In both seasons, deep convection is less frequent; however, intense evaporatively driven downdrafts often occur associated with squall lines (Garstang et al. 1998; Juárez et al. 2010). Downdraft wind gusts of up to 15 m s^{-1}, the largest natural perturbation to the antenna to be expected, were in fact recorded during the experiment.

b. Study sites

The 55-m-high LBA K34 flux tower, 60 km to the north-northwest of Manaus (2.699°S, 60.159°W) has provided a wealth of data on fluxes of energy and trace gases (e.g., Araújo et al. 2002). During the flux tower phase of the experiment, the GNSS (designated RBDC) antenna was extended from the tower on a 2-m aluminum tube to minimize obstructions and multipath, but also to amplify oscillations in the horizontal and vertical plane (Fig. 1 and inset) creating a ''worst case scenario'' for rain forest flux tower conditions in terms of oscillations. Semiregular, wind-forced (~3 m s^{-1} in undisturbed conditions and greater than 10 m s^{-1} during convective downdrafts) and irregular technician- or researcher-induced oscillations were continuously experienced by the antenna. We expect that oscillations reached several centimeters in the vertical plane and an amplitude greater than 5 cm in the horizontal. The GNSS site at INPA in Manaus (3.097°S, 59.989°W), part of the National Oceanic and Atmospheric Administration/Earth System Research Laboratory (NOAA/ESRL) Ground-Based GPS Meteorological Network, served as the stable reference. For the second experimental phase, RBDC was removed (and redesignated INPB) from the flux tower and placed on the oscillating device 1.5 m horizontally and 0.35 m vertically from the INPA antenna. At this distance, no physically significant difference in PWV is measurable; therefore, any divergence in PWV values is due to equipment, processing techniques, and/or antenna oscillations. Twice-daily radiosondes (Sippican Mark IIA) released from station SBMN (82332) (3.15°S, 59.98°W), approximately 5 km from INPA, provided independent PWV data for comparison.

c. Data

Two different dual-frequency, L1 (λ = 0.1903 m) and L2 (λ = 0.244 m), geodetic-grade GNSS receivers/antennas were employed; the Trimble NetRS/Trimble Zephyr Geodetic (INPA) and the Topcon GB1000/Topcon PG-A1 (RBDC and INPB). Typically, 10 to 12 GPS satellites were in view for both receivers at all times. The GAMIT software package (King and Bock 2005) is employed by NOAA/ESRL to estimate INPA station zenith total delay in near–real time. PWV is calculated every 15 and 45 min after the hour and is available online at http://gpsmet.noaa.gov/test/cgi-bin/gnuplots/rti.cgi. GIPSY software (Webb and Zumberge 1993) was utilized for processing all data (RBDC, INPB, and INPA stations) at 5-min intervals using the Precise Point Positioning (PPP) strategy. Details of the GIPSY processing are described in Fernandes et al. (2006). In the second experiment, INPB was mechanically oscillated with amplitudes ranging from 8 to 12 cm in the horizontal and 1 cm in the vertical and at frequencies varying between 0.7 and 0.25 Hz. Initially, INPB remained rigidly fixed for comparison with INPA. Afterward, various INPB

FIG. 1. The 55-m LBA meteorological flux tower K34, located in Amazon rain forest 60 km northwest of Manaus, Amazonas, Brazil. Photo (lower left) was taken prior to placement of any meteorological and flux equipment. Tower extends approximately 15 m above forest canopy. Yellow GNSS antenna (RBDC) on 2-m aluminum tube extends from the side of the tower (inset photo).

Table 1. Naming conventions for instruments and experimental design. Four-character designation (RBDC, INPB, INPA, and SBMN) is solely for identification purposes of each site following standard GNSS naming conventions. The location of INPB is separated from INPA by 1.5 m in the horizontal and 35 cm in the vertical. Dates are represented as decimal days and continuous data were available for all of 2009.

ID	Location	Equipment	Processing	Dates
RBDC	2.699°S, 60.159°W	Topcon GB1000	GIPSY	194–247
INPB	3.097°S, 59.989°W	Topcon GB1000	GIPSY	311–332
INPA GAMIT	3.097°S, 59.989°W	Trimble NetRS	GAMIT	Continuous
INPA GIPSY	3.097°S, 59.989°W	Trimble NetRS	GIPSY	Continuous
SBMN	3.150°S, 59.989°W	Sippican Mark II	N/A	Continuous

configurations of the above-mentioned amplitudes and frequencies were applied for periods ranging from 12 h to several days. Table 1 summarizes the naming convention and experimental details.

4. Results and discussion

a. *Rain forest flux tower*

The PWV time series for RBDC, INPA GAMIT, INPA GIPSY, and SBMN from the first experiment are presented in Fig. 2. It is apparent that on time scales longer than 12 h, the different GNSS PWV values are qualitatively consistent irrespective of equipment or processing methodology. Root-mean-square errors (rmse) between RBDC and both INPA GAMIT and INPA GIPSY are 2.2 and 2.5 mm, respectively, with deviations greater than 6 mm for some individual time steps. Rmse between RBDC and the SBMN radiosonde is large at 3.7 mm with GNSS slightly overestimating PWV relative to the sondes (Bias = 0.7 mm). These results are nearly identical to those from previous studies in Amazonia (Sapucci et al. 2007). Gauging from these results, accurate PWV values are achieved even from a highly nonideal rain forest platforms. However, at 60-km separation, mesoscale variability in water vapor fields should account for observed differences, not equipment and/or processing. To confirm this, the second experiment was carried out.

b. *Collocated receivers: Stable and oscillating configurations*

To ascertain PWV differences attributable solely to equipment and/or processing methods, the Topcon receiver/antenna (INPB) was placed next to INPA from decimal day 311 to 317 in a rigid configuration. From day 318 to 333, INPB oscillated at different frequencies and amplitudes mimicking K34 flux tower oscillations. Figure 3 plots INPA (both GIPSY and GAMIT), INPB and SBMN radiosondes PWV. Mesoscale variability is absent and the different GNSS processing methods compare quite well between the stable and oscillating configurations. For direct comparison of equipment and processing methods, the stable period was analyzed (upper graphic, Fig. 4). For equipment comparison, PWV was calculated for INPA and INPB using GIPSY processing alone. Results for this small sample period ($N = 1575$) show an rmse of 0.74 mm and a wet bias (Trimble > Topcon) of 0.53 mm. Extending the comparison to include the INPB oscillating period ($N = 4459$) (lower graphic, Fig. 4), the rmse remains the same; however, the Trimble wet bias increases to 0.78 mm. From this figure, the changing of the amplitude or the frequency of oscillation of INPB has no obvious consequences in terms of the bias. SBMN sonde PWV compared over the entire period (311–333) has a large rmse of 4.4 mm and a dry bias of 0.9 mm; however, the sample size is small ($N = 42$): an rmse of 5.2 mm and dry bias of 0.2 mm and an rmse of 4.1 mm and a dry bias of 0.8 mm during the stationary ($N = 28$) and oscillating ($N = 14$) periods, respectively.

For the purpose of direct comparison of processing techniques alone, much more robust statistics can be calculated for all of 2009 with INPA station data. In this case, GAMIT PWV, calculated every 30 min by NOAA/ESRL, is compared with the corresponding instantaneous GIPSY PWV values, calculated every 5 min. That is, no smoothing was applied to the GIPSY processing in this comparison. For all of 2009, ($N = 10\,531$), GAMIT/GIPSY PWV has an rmse of 0.95 mm and a very small bias (0.11 mm, GAMIT PWV > GIPSY PWV). The nearly 1-mm rmse between the two methods does not appear to result from noisier higher time resolution GIPSY processing. GIPSY PWV values averaged over 30 min centered on the GAMIT values provide exactly the same rmse with only a minimal decrease in bias (0.10 mm, GAMIT PWV > GIPSY PWV).

For this study, the most "nonideal" arrangement, an unstable platform, different equipment, and processing, is represented by INPA GAMIT and INPB (see Fig. 3) during the oscillating period. Not surprisingly, the errors are larger ($N = 701$) (rmse = 1.4 mm) with a bias of 1.3 mm (INPA GAMIT PWV > INPB PWV). Considering the above results between GAMIT and GIPSY, the positive bias is entirely consistent for Trimble versus Topcon. Again, the INPB oscillations seem to have only minimal effects on the error: rmse = 1.4 mm with a bias

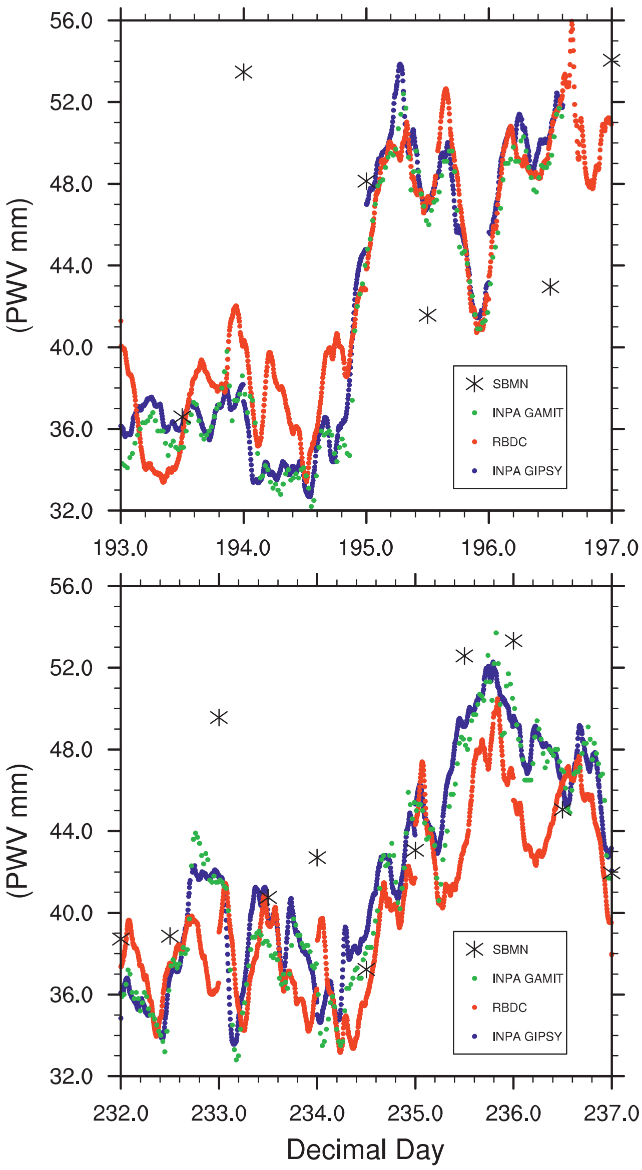

FIG. 2. Times series of PWV values for two periods for which all data were available (decimal days 193–197 and 232–237). Red dots represent 5-min GIPSY processing for RBDC, green dots represent 30-min GAMIT processing for INPA, blue dots represent 5-min GIPSY processing for INPA, and black asterisks represent twice-daily radiosondes, SBMN.

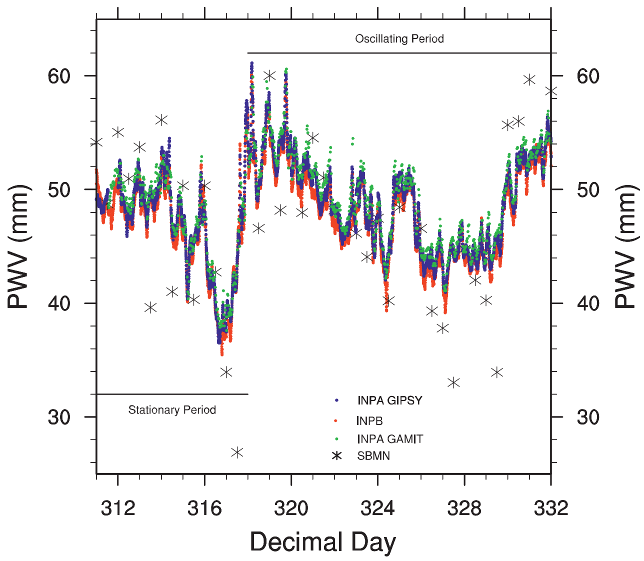

FIG. 3. Time series of PWV values for INPB (red dots), in both stationary (decimal days 311–317) and oscillating configurations (decimal days 318–332) and INPA, processed using GIPSY (blue dots) and GAMIT (green dots). Black asterisks represent twice-daily radiosondes, SBMN.

of 1.0 mm for $N = 310$ for the nonoscillating period. Although there are many sources of error in the GNSS technique itself, these small errors are probably due to oscillations are mostly due to changes with time in the position of the antenna phase center.

To summarize briefly, the rmse as large as 2.5 mm observed during the flux tower experiment, though not large in absolute terms, is most likely the result of mesoscale variability in water vapor. The rmse of well less than 1 mm during the stable configuration of the second experiment supports this contention. Our best "error" estimate associated with nonideal oscillating conditions, free from mesoscale variability, gives an rmse of greater than 1 mm, which is approximately 2%. With respect to equipment and processing analyses, the only clearly consistent result was a small positive (wet) bias of the Trimble over the Topcon of 0.53 mm. However, given that not all combinations of equipment and processing were available, it is not possible to attribute conclusively the differences in observed PWV to either processing or equipment.

5. Conclusions and future work

Accurate PWV measures from such nonideal sites open up the possibility to extend GNSS meteorology into remote, logistically challenging regions such as deep tropical rain forest where water vapor values are critical to all aspects of the climate system. At present, approximately 14 above-canopy flux towers are scattered throughout the Amazon (A. Araújo 2010, personal communication) and could in principle serve as continuous PWV sites. Furthermore, the 300-m meteorological Amazonian Tall Tower Observatory (ATTO), to be constructed in the Amazon (http://www.nature.com/news/2010/100922/pdf/467386a.pdf), would offer a unique opportunity to examine rain forest boundary layer development with receivers placed at the tower top and surface. Given our results, we are emboldened to locate GNSS meteorological stations in highly undesirable locales of limited sky views and proximity to powerful

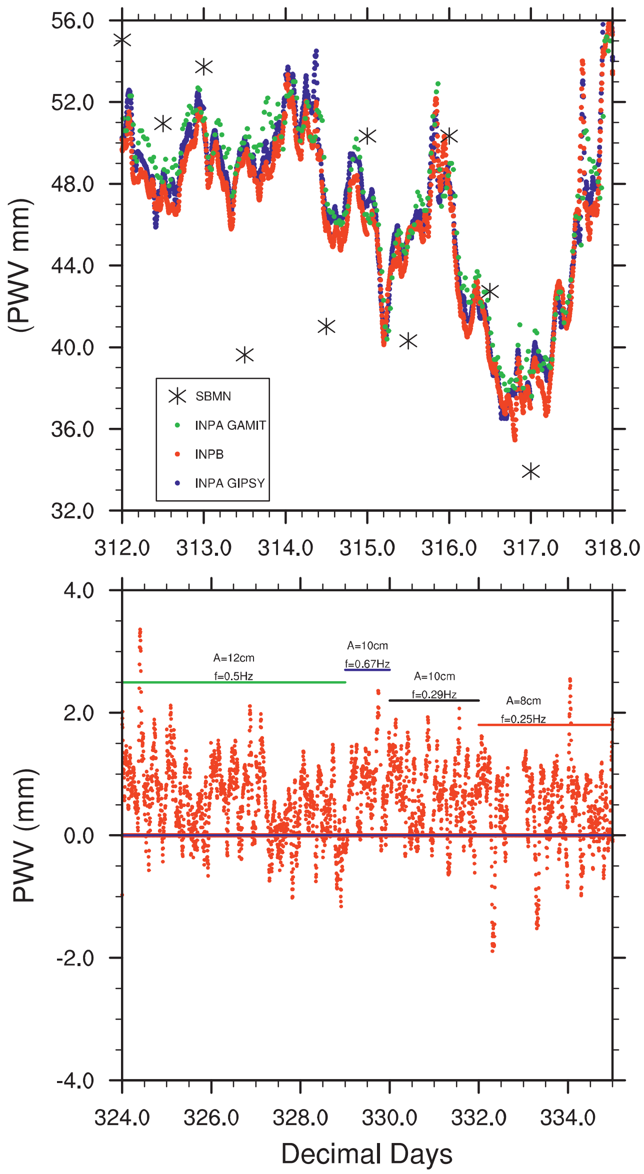

FIG. 4. (top) Enlarged figure (cf. Fig. 3) of PWV time series for INPB during stationary period (decimal days 311–317). (bottom) (cf. Fig. 3) Difference in PWV between INPA and INPB (both GIPSY processed) during oscillating phase of the experiment (decimal days 318–332) with colored lines representing the length of the oscillation period.

emitting antennas. If results are accurate and receiver costs decrease, GNSS meteorology may become even more feasible, which would be of particular benefit for the creation of smaller-scale networks where highly nonideal sites are often a necessity.

Acknowledgments. We thank Dr. Antônio Manzi of the INPA/LBA for financial support of this project. Thanks go to Seth Gutman, Earl Williams, and an anonymous reviewer for critical reading of the manuscript. We appreciate Thiago de Lima's data collection and data supplied by the INPA/LBA Micrometeorology group (Alessandro Araújo, Leila Leal, Marta Sá). We thank Kirk Holub (NOAA), Rick Bennett (University of Arizona), and UNAVCO for technical support. Support for this project and the Amazonian Dense GNSS Network comes through Cooperation Project 0050.0045370.08.4 between PETROBRAS and INPE and KINEMA (PTDC/CTE-GIN/64101/2006) project funded by the Portuguese Fundação para a Ciência e Tecnologia.

REFERENCES

Adams, D. K., and E. Souza, 2009: CAPE and convective events in the Southwest during the North American monsoon. *Mon. Wea. Rev.*, **137,** 83–89.

——, E. R. Kursinski, and R. A. Bennett, 2009: GPS observations of precipitable water vapor in deep convective tropical regimes. *Proc. AIP Conf. on Current Problems in Atmospheric Radiation (IRS 2008),* American Institute of Physics, Melville, NY, 207–210.

——, and Coauthors, 2011: A dense GNSS meteorological network for observing deep convection in the Amazon. *Atmos. Sci. Lett.,* **12,** 207–212, doi:10.1002/asl.312.

Araújo, A. C., and Coauthors, 2002: Comparative measurements of carbon dioxide fluxes from two nearby towers in a central Amazonian rainforest: The Manaus LBA site. *J. Geophys. Res.,* **107,** 8090, doi:10.1029/2001JD000676.

Bastin, S., C. Champollion, O. Bock, P. Drobinski, and F. Masson, 2007: Diurnal cycle of water vapor as documented by a dense GPS network in a coastal area during ESCOMPTE IOP2. *J. Appl. Meteor. Climatol.,* **46,** 167–182.

Bechtold, P., J. Chaboureau, A. Beljaars, A. Betts, M. Kohler, M. Miller, and J. Redelsperger, 2004: The simulation of the diurnal cycle of convective precipitation over land in a global model. *Quart. J. Roy. Meteor. Soc.,* **130,** 3119–3137.

Bender, M., and A. Raabe, 2007: Preconditions to ground-based water vapour tomography. *Ann. Geophys.,* **25,** 1727–1734.

Betts, A. K., and C. Jakob, 2002: Study of diurnal convective precipitation over Amazonia using a single column model. *J. Geophys. Res.,* **107,** 4732, doi:10.1029/2002JD002264.

Bevis, M., S. Businger, T. A. Herring, C. Rocken, R. Anthes, and R. H. Ware, 1992: GPS meteorology: Sensing of atmospheric water vapor using the global positioning system. *J. Geophys. Res.,* **97,** 15 787–15 801.

Braun, J., C. Rocken, and R. Ware, 2001: Validation of line-of-site water vapor measurements with GPS. *Radio Sci.,* **36,** 459–472.

Chadwell, C. D., and Y. Bock, 2001: Direct estimation of absolute precipitable water in oceanic regions by GPS tracking of a coastal buoy. *Geophys. Res. Lett.,* **28,** 3701–3704.

Champollion, C., F. Masson, M.-N. Bouin, A. Walpersdorf, E. Doerflinger, O. Bock, and J. van Baelen, 2005: GPS water vapor tomography: Preliminary results from the ESCOMPTE field experiment. *Atmos. Res.,* **74,** 253–274.

——, C. Flamant, O. Bock, F. Masson, D. D. Turner, and T. Weckwerth, 2009: Mesoscale GPS tomography applied to the 12 June 2002 convective initiation event of IHOP_2002. *Quart. J. Roy. Meteor. Soc.,* **135,** 645–662.

Deeter, M., 2007: A new satellite retrieval method for precipitable water vapor over land and ocean. *Geophys. Res. Lett.,* **34,** L02815, doi:10.1029/2006GL028019.

Divakarla, M. G., C. D. Barnet, M. D. Goldberg, L. M. McMillin, E. Maddy, W. Wolf, L. Zhou, and X. Liu, 2006: Validation of Atmospheric Infrared Sounder temperature and water vapor retrievals with matched radiosonde measurements and forecasts. *J. Geophys. Res.,* **111,** D09S15, doi:10.1029/2005JD006116.

Duan, J., and Coauthors, 1996: GPS meteorology: Direct estimation of the absolute value of precipitable water. *J. Appl. Meteor.,* **35,** 830–838.

Emanuel, K. A., 1991: A scheme for representing cumulus convection in large-scale models. *J. Atmos. Sci.,* **48,** 2313–2329.

Fernandes, R. M. S., L. Bastos, J. M. Miranda, N. Lourenço, B. A. C. Ambrosius, R. Noomen, and W. Simons, 2006: Defining the plate boundaries in the Azores region. *J. Volcanol. Geotherm. Res.,* **156,** 1–9.

Flores, A., J. V.-G. de Arellano, L. Gradinarsky, and A. Rius, 2001: Tomography of the lower troposphere using a small dense network of GPS receivers. *IEEE Trans. Geosci. Remote Sens.,* **39,** 439–447.

Fujita, M., F. Kimura, K. Yoneyama, and M. Yoshizaki, 2008: Verification of precipitable water vapor estimated from shipborne GPS measurements. *Geophys. Res. Lett.,* **35,** L13803, doi:10.1029/2008GL033764.

Garstang, M., S. White, H. Shugart, and J. Halverson, 1998: Convective cloud downdrafts as the cause of large blowdowns in the Amazon rainforest. *Meteor. Atmos. Phys.,* **67,** 199–212, doi:10.1007/BF01277510.

Grabowski, W. W., and M. W. Moncrieff, 2004: Moisture-convection feedback in the tropics. *Quart. J. Roy. Meteor. Soc.,* **130,** 3081–3104.

——, and Coauthors, 2006: Daytime convective development over land: A model intercomparison based on LBA observations. *Quart. J. Roy. Meteor. Soc.,* **132,** 317–344.

Gutman, S. I., S. R. Sahm, S. G. Benjamin, and B. E. Schwartz, 2004: Rapid retrieval and assimilation of ground-based GPS precipitable water observations at the NOAA Forecast Systems Laboratory: Impact on weather forecasts. *J. Meteor. Soc. Japan,* **82,** 351–360.

James, R. P., and P. M. Markowski, 2010: A numerical investigation of the effects of dry air aloft on deep convection. *Mon. Wea. Rev.,* **138,** 140–161.

Juárez, R. I. N., and Coauthors, 2010: Widespread Amazon forest tree mortality from a single cross-basin squall line event. *Geophys. Res. Lett.,* **37,** L16701, doi:10.1029/2010GL043733.

Khairoutdinov, M., and D. Randall, 2006: High-resolution simulation of shallow-to-deep convection transition over land. *J. Atmos. Sci.,* **63,** 3421–3436.

King, R. W., and Y. Bock, 2005: Documentation for the GAMIT GPS processing software release 10.2. Massachusetts Institute of Technology.

Kuang, Z., and C. S. Bretherton, 2006: A mass-flux scheme view of a high-resolution simulation of a transition from shallow to deep cumulus convection. *J. Atmos. Sci.,* **63,** 1895–1909.

Kursinski, E. R., and Coauthors, 2008: Water vapor and surface observations in northwestern Mexico during the 2004 NAME Enhanced Observing Period. *Geophys. Res. Lett.,* **35,** L03815, doi:10.1029/2007GL031404.

Mapes, B. E., and P. Zuidema, 1996: Radiative-dynamical consequences of dry tongues in the tropical troposphere. *J. Atmos. Sci.,* **53,** 620–638.

Muller, C. J., L. E. Back, P. A. O'Gorman, and K. A. Emanuel, 2009: A model for the relationship between tropical precipitation and column water vapor. *Geophys. Res. Lett.,* **36,** L16804, doi:10.1029/2009GL039667.

Parsons, D. B., K. Yoneyama, and J. L. Redelsperger, 2000: The evolution of the tropical western Pacific atmosphere-ocean system following the arrival of a dry intrusion. *Quart. J. Roy. Meteor. Soc.,* **126,** 517–548.

Peters, O., and J. D. Neelin, 2009: Mesoscale convective systems and critical clusters. *J. Atmos. Sci.,* **66,** 2913–2924.

Roca, R., J.-P. Lafore, C. Piriou, and J.-L. Redelsperger, 2005: Extratropical dry-air intrusions into the west African monsoon midtroposphere: An important factor for the convective activity over the Sahel. *J. Atmos. Sci.,* **62,** 390–407.

Rocken, C., R. H. Ware, T. V. Hove, F. Solheim, C. Alber, J. Johnson, M. Bevis, and S. Businger, 1993: Sensing atmospheric water vapor with the Global Positioning System. *Geophys. Res. Lett.,* **20,** 2631–2634.

——, J. Johnson, T. V. Hove, and T. Iwabuchi, 2005: Atmospheric water vapor and geoid measurements in the open ocean with GPS. *Geophys. Res. Lett.,* **32,** L12813, doi:10.1029/2005GL022573.

Sapucci, L. F., L. A. T. Machado, J. F. G. Monico, and A. Plana-Fattori, 2007: Intercomparison of integrated water vapor estimates from multisensors in the Amazonian region. *J. Atmos. Oceanic Technol.,* **24,** 1880–1894.

Seko, H., H. Nakamura, Y. Shoji, and T. Iwabuchi, 2004: The meso-γ scale water vapor distribution associated with a thunderstorm calculated from a dense network of GPS receivers. *J. Meteor. Soc. Japan,* **82,** 569–586.

Sherwood, S., 1999: Convective precursors and predictability in the tropical Western Pacific. *Mon. Wea. Rev.,* **127,** 2977–2991.

——, R. Roca, T. Weckwerth, and N. Andronova, 2009: Tropospheric water vapor, convection and climate: A critical review. *Rev. Geophys.,* **48,** RG2001, doi:10.1029/2009RG000301.

Silva-Dias, M. S., and Coauthors, 2002: Cloud and rain processes in a biosphere–atmosphere interaction context in the Amazon region. *J. Geophys. Res.,* **107,** 8072, doi:10.1029/2001JD000335.

Smith, T. L., S. Benjamin, S. I. Gutman, and S. Sahm, 2007: Short-range forecast impact from assimilation of GPS-IPW observations into the rapid update cycle. *Mon. Wea. Rev.,* **135,** 2914–2930.

Webb, F. H., and J. F. Zumberge, 1993: An introduction to the GIPSY/OASIS-II. Publ. d-11088, Jet Propulsion Laboratory, 300 pp.

Williams, E., and N. Rennó, 1993: An analysis of the conditional instability of the tropical atmosphere. *Mon. Wea. Rev.,* **121,** 21–36.

Wolfe, D. E., and S. I. Gutman, 2000: Developing an operational, surface-based, GPS, water vapor observing system for NOAA: Network design and results. *J. Atmos. Oceanic Technol.,* **17,** 426–440.

Wu, C.-M., B. Stevens, and A. Arakawa, 2009: What controls the transition from shallow to deep convection? *J. Atmos. Sci.,* **66,** 1793–1806.